Assessment of the Aerosol Optics Component of the Coupled WRF-CMAQ Model using CARES Field Campaign data and a Single Column Model

Chuen Meei Gan[1], Francis Binkowski[2], Jonathan Pleim[1], Jia Xing[1], David Wong[1], Rohit Mathur[1] and Robert Gilliam[1]

(1) Atmospheric Modeling and Analysis Division, National Exposure Research Laboratory, US Environmental Protection Agency, Research Triangle Park, North Carolina, USA

(2) Center for Environmental Modeling for Policy Development, The University of North Carolina at Chapel Hill, North Carolina USA

Corresponding author: Chuen-Meei Gan, AMAD, NERL, US EPA (chuenmeei@gmail.com, Gan.Meei@epa.gov).

Abstract

The Carbonaceous Aerosols and Radiative Effects Study (CARES), a field campaign held in central California in June 2010, provides a unique opportunity to assess the aerosol optics modeling component of the two-way coupled Weather Research and Forecasting (WRF) – Community Multiscale Air Quality (CMAQ) model. This campaign included comprehensive measurements of aerosol composition and optical properties at two ground sites and aloft from instrumentation on-board two aircraft. A single column model (SCM) was developed to evaluate the accuracy and consistency of the coupled model using both observation and model information. Two cases (June 14 and 24, 2010) are examined in this study. The results show that though the coupled WRF-CMAQ estimates of aerosol extinction were underestimated relative to these measurements, when measured concentrations and characteristics of ambient aerosols were used as input to constrain the SCM calculations, the estimated extinction profiles agreed well with aircraft observations. One of the possible causes of the WRF-CMAQ extinction errors is that the simulated sea-salt (SS) in the accumulation mode in WRF-CMAQ is very low in both cases while the observations indicate a considerable amount of SS. Also, a significant amount of organic carbon (OC) is present in the measurement. However, in the current WRF-CMAQ model all OC is considered to be insoluble whereas most secondary organic aerosol is water soluble. In addition, the model does not consider external mixing and hygroscopic effects of water soluble OC which can impact the extinction calculations. In conclusion, the constrained SCM results indicate that the scattering portion of the aerosol optics calculations is working well, although the absorption calculation could not be effectively evaluated. However, a few factors such as greatly underestimated accumulation mode SS, misrepresentation of water soluble OC, and incomplete mixing state representation in the full coupled model simulation are possible causes of the underestimated extinction. Improved SS emission modeling and revisions to more fully account for OC in the optical calculations are being pursued. More sensitivity tests related to the factors mentioned previously are needed for future optical properties development.

1 Introduction

Many studies in the past have utilized observations to evaluate the key components of atmospheric models (e.g. aerosol optical properties, radiation and meteorology) [Mebust et al. 2003; Schmid et al. 2006; Michalsky et al. 2006; Roy et al. 2007 and Mathur, 2008]. However, it is still a challenge to obtain comprehensive and high quality measurements to diagnose the model in every aspect. The Carbonaceous Aerosols and Radiative Effects Study (CARES) [Zaveri et al. 2012], which was sponsored by the United State Department of Energy (DOE), is one of the few campaigns that made comprehensive measurement suites at two ground sites and on two aircraft platforms providing continuous information on the evolution of meteorological variables, trace gases, aerosol size, composition, optical properties, solar radiation and cloud condensation nuclei activation properties. The CARES campaign, from 2 - 28 June 2010 provides an opportunity to conduct an intensive evaluation for the two-way coupled Weather Research and Forecasting (WRF) – Community Multiscale Air Quality (CMAQ) model [Wong et al. 2012]. The WRF-CMAQ model is being increasingly applied to studies of air pollution and human health so it is important to improve the overall model performance.

In this study, we not only assess the coupled model directly by comparing predictions with observations but also examine the aerosol optics parameterization by running a single column model (SCM; that emulates the aerosol optics calculations of WRF-CMAQ) with inputs based on both modeled and observed aerosol concentrations, compositions, and sizes distributions. Comparing SCM extinction profiles to aircraft measurements provides insights into the model accuracy and consistency. Several sensitivity tests are conducted to diagnose model-observed discrepancies and devise the possible solutions to improve the model. A brief description of the coupled WRF-CMAQ model and field campaign is given in Section 2. Section 3 gives the details of the SCM and methodology which is used in this study. The results from two cases studies are presented in Section 4 followed by conclusions in Section 5.

2. Data descriptions

2.1 Coupled WRF-CMAQ model

The two-way WRF-CMAQ model simulations were performed with WRFv3.4 and CMAQv5.02. For this study the modeling domain covering California (see Figure 1) is discretized with grid cells of 4 km by 4 km in the horizontal and with 34 vertical layers of varying thickness in the vertical (between the surface and 50 mb). The simulation period is from May 4 to June 30, 2010. The details of the model parameterizations are listed in Table 1.

The several modifications had been made to the two-way coupled model such as densities and refractive indices (RI) for different particulate matter species [Hess et al. 1998 and Chen & Bond 2010]. The Mie (BHMIE) homogeneous internal mixing and the core-shell (BHCOAT) homogeneous shell mixing with element carbon in the core approaches from Bohren and Huffman [1998] are used. In the model, we integrate BHMIE and BHCOAT over the particle log-normal size distributions. This is done by using Gauss-Hermite numerical quadrature involving carefully constructed complex arithmetic algorithms to preserve numerical precision while having computational efficiency.

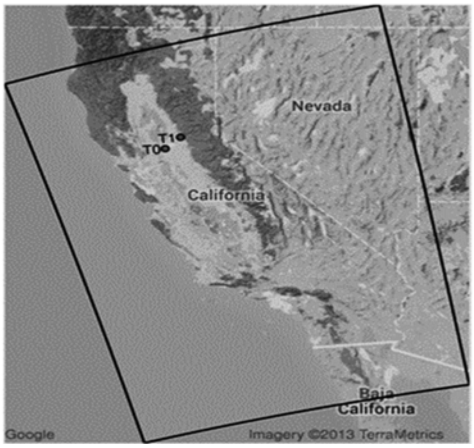

Figure 1: Location of the supersites, T0, Sacramento, CA (urban area) [elevation = 9 m, latitude = 38.55°, longitude = -121.47°] and T1, Cool, CA (~40 km downwind in the forested Sierra Nevada foothills area) [elevation = 467 m, latitude = 38.88°, longitude = -121.02°]. The straight line distance between the two sites is approximate 53 km.

Table 1 Model configuration

Category	**Description**
Planetary Boundary Layer	ACM2
Microphysics	Morrison 2-moment scheme
Gas-Phase Chemistry	Carbon Bond 05
Aerosol Chemistry	AERO6
Land Surface	Pleim-Xiu
Cumulus	Kain-Fritsch
Radiation	RRTMG
Mobile Temporal Profile	EPA
Land Use	NLCD/MODIS
Boundary Conditions	GEOS-Chem v8-03-02
Onroad/nonroad emission	Interpolated from CARB’s 2007 and 2011 totals
Point source emission	2010 data
Grid cell size	4 km
Output Temporal resolution	1 hour for two months and 6 minutes for study cases

2.2 Field Campaign description

This assessment is to evaluate the improved aerosol component of the two-way coupled WRF-CMAQ model mainly in representing aerosol physical and optical properties by utilizing observations from the CARES [http://campaign.arm.gov/cares/] during June 2010 in central California (CA). The objective of the CARES was to investigate the evolution of carbonaceous aerosols of different types and their optical and hygroscopic properties. Several recent studies have analyzed the in-situ measurements from a range of instruments (e.g. AMS, PSAP and FIMS) together with those deployed aboard two aircraft (DOE G-1 and NASA B-200) during the field campaign [Setyan et al., 2012; Cahill et al., 2012; Kassianov et al., 2012; Shilling et al, 2013; Kelly et al., 2014; and Fast et al., 2014] to address a range of scientific questions. Here, measurements of particulate matter size, composition, and optical properties at the surface and aloft are used to assess both the full 3-d coupled WRF-CMAQ and SCM results. Measurements from the aircraft and supersites (T0 and T1) are combined and used in the SCM assessment to evaluate the accuracy of the aerosol optical properties estimated by WRF-CMAQ. Figure 1 shows the supersites locations, T0 near Sacramento and T1 is near Cool. The details of the campaign and list of measurements can be found at http://campaign.arm.gov/cares/ and Zaveri et al [2012]. The post-processed data can also be downloaded from Aerosol Modeling Testbed (AMT) (Fast et al, 2011; Fast et al., 2012) at https://www.arm.gov/data/eval/59.

The main observations used in this study are (a) the size distribution measurements made by Fast Integrating Mobility Spectrometer (FIMS) (Kulkarni and Wang, 2006a and 2006b), Ultra High Sensitivity Aerosol Spectrometer (UHSAS) (Cai et al., 2008) and Cloud, Aerosol and Precipitation Spectrometer (CAPS) (Baumgardner et al., 2001); (b) species information made by Aerosol Mass Spectrometer (AMS) (Bahreini et al., 2009; Canagaratna et al., 2007; Middlebrook et al., 2012), Particle Liquid Sampler (PILS) (Weber et al., 2001) and Single Particle Soot Photometer (SP2) (Metcalf et al., 2012; Langridge et al., 2012; Laborde et al.,, 2012) and (c) aerosol extinction based on nephelometer (neph) (Massoli et al., 2009; Müller et al., 2011) and particle soot absorption photometer (PSAP) (Bond et al., 1999) measurements. Note that each of measurements (i.e. direct measurement or retrieval with some assumptions) has its own systematic errors and uncertainties, and are used as a reference to verify and constrain model assessments.

The single scattering albedo (SSA), the ratio of scattering coefficient to total extinction coefficient, at 550 nm wavelength is used in subsequent analysis can be calculated based on aerosol extinction using equation 1 below:

$$SSA = \frac{\beta_{sca}(\lambda)}{\beta_{sca}(\lambda)+\beta_{abs}(\lambda)} \qquad \text{Equation 1}$$

where $\beta_{sca}(\lambda)$ is the scattering coefficient, $\beta_{abs}(\lambda)$ is the absorption coefficient, $\beta_{ext}(\lambda)$ is the sum of scattering and absorption coefficients and λ is the wavelength. Because $\beta_{sca}(\lambda)$ and $\beta_{abs}(\lambda)$ depend upon the RI of the constituent species as well as wavelength, we emphasize that SSA has the same dependencies. These data, which had been quality inspected, are retrieved and delivered directly from the AMT / CARES team. Equation 1 is provided to briefly explain the SSA calculation but the detail retrieval procedures and its uncertainty were not given by Project Investigator.

Because each instrumental system has its own unique protocol for processing, some assumptions needed to be invoked to combine these measurements. For example, different instruments measure different size ranges with diverse resolution albeit with some overlap in size. In order to develop a consistent dataset across the larger size spectrum, we took the average of both measurements in the overlap region and then interpolated the data to regenerate a uniform dataset. Also, since the particle size diameter provided can be the aerodynamic diameter or mobility diameter, it is important to convert one of them before the data fusion.

3. Single Column Model (SCM)

One of the objectives of this study is to evaluate the aerosol component of the coupled WRF-CMAQ model [Binkowski et al. 1999 and 2003], particularly the physical and optical aspects by using a SCM. This SCM was configured to use 35 layers in the vertical extending from the surface to 50 hPA. The SCM is designed to read in a vertical profile of aerosol properties either from observations or from the coupled WRF-CMAQ model. The SCM then calculates a vertical profile of aerosol optical depth (AOD) based on the same extinction parameterization used in the CMAQ aerosol module algorithms. Profiles of SSA are also calculated within the SCM.

In order to provide values above 3 km, a set of profile calculations using the widely accepted Mid-Latitude-Summer (MLS) [vanWeele et al., 2000; Clough et al., 2012 and Bani Shahabadi et al., 2014] case supplemented the observations as the aircraft flying altitude is limited to below 3 km. The temperature, pressure and relative humidity (RH) from the observations were used to represent the environment between the surface and 3 km. The observed aerosol information was mapped into the five lumped model species in the coupled WRF-CMAQ model. These are water-soluble (WS), insoluble (IN), sea-salt (SS), elemental-carbon (EC), and water. Details of the methodology for generating input profiles from observation and model are described in the following section.

3.1 Methodology

The overall approach for processing measurement data to be used as input for the SCM is shown in Figure 2. First, the aircraft data are filtered by the type of flight path and the completeness of the measurements. For example, the vertical profiles need to be completed in one time frame and should not span a large horizontal distance (see examples of such spirals in Figures 3 and 13). The second requirement is that the profiles must have concurrent measurements of all required aerosol composition, size and optical properties. For instance, if one of the instruments for measuring particle number concentration was not functioning properly or there was missing partial data, the other measurements cannot be used either. Note that, most of the aircraft measurements were in the 0.5-3 km altitude range during this campaign.

After selecting the vertical profiles, the measurements of number of particles in different size ranges for each layer are combined by matching their diameter bins. As mentioned above, the size discriminated average number concentration (i.e. dN/dlogDp) is obtained for the diameter overlap region. Since the bin sizes are not the same for each instrument, the data are interpolated to a uniform diameter bin size dataset.

Next, measurements of AMS, PILS and SP2 are combined to obtain aerosol composition in the vertical direction. The aerosol species considered in the study include: sodium (Na), sulfate (SO_4^{2-}), ammonium (NH_4^+), nitrate (NO_3^-), chloride (Cl^-), potassium (K^+), magnesium (Mg^{2+}), calcium (Ca^{2+}), element carbon (EC) and organic carbon (OC). Before they are apportioned into Aitken, accumulation and coarse modes, the aircraft composition measurements (lowest layer) is compared to the surface composition measurements to ensure the consistency. Since the aircraft has a very fine temporal resolution, the speciated mass measurements are averaged into 100 m vertical resolution bins. The aerosol water content is computed with ISORROPPIA (Nenes et al. 1998a and 1998b) using the observed particulate composition and RH measurements. Note that ISORROPIA is used for inorganic species thermodynamic equilibrium thus in these calculations, hygroscopic effects on water soluble OC is not considered.

These datasets are then grouped into three categories: WS, EC and SS for each model size mode (i.e. Aitken, accumulation and coarse) using equations 2-4, 6-9 and 11-13. For example, in the accumulation mode, the WS from observation (obs) and model are computed with equations 6 and 7, respectively while SS uses equation 9 for both. Note that, IN is only considered in the coupled model derived input SCM test because there is no insoluble aerosol species measurement available in this study. Also, the observed OC is assumed as water soluble organic.

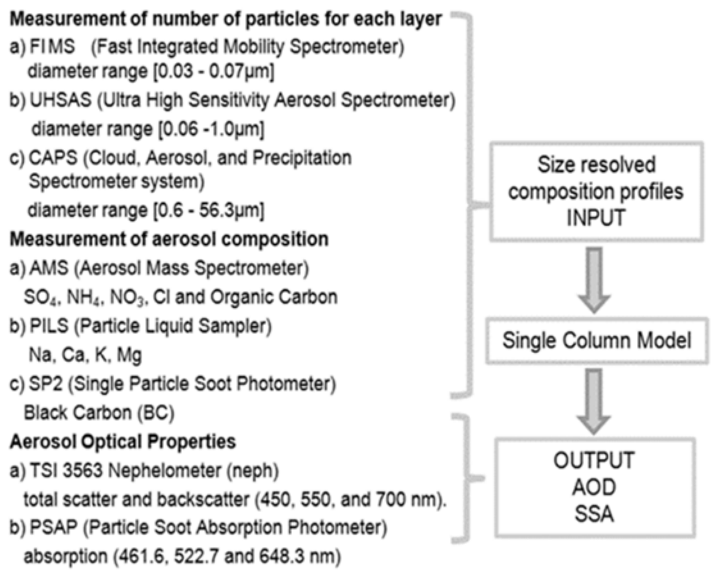

Figure 2: Flow chart of data processing for Single Column Model

Aitken (atk) Mode:

$WS_{obs\_atk/model\_atk} = SO_4 + NH_4 + NO_3$ Equation 2

$EC_{obs\_atk/model\_atk} = EC$ Equation 3

$SS_{obs\_atk/model\_atk} = 0.0$ Equation 4

IN_{model_atk} = Primary OC + Other + Primary Non-carbon organic Equation 5

Accumulation (acc) Mode:

$WS_{obs\_acc} = SO_4 + NH_4 + NO_3 + Mg + K + Ca + OC$ Equation 6

$WS_{model\_acc} = SO_4 + NH_4 + NO_3 + Mg + K + Ca$ Equation 7

$EC_{obs\_acc/model\_acc} = EC$ Equation 8

$SS_{obs\_acc/model\_acc} = Na + Cl$ Equation 9

IN_{model_acc} = "Alkane + Toluene + Benzene + Other Anthropogenic" SOA + Primary OC + Monoterpene + Isoprene + Sesquiterpene + Biogenic SOA + Other + Primary non-Carbon Organic + Fe + Al + Si + Ti + Mn Equation 10

Coarse (coa) Mode:

$WS_{obs\_coa/model\_coa} = 0.0$ Equation 11

$EC_{obs\_coa/model\_coa} = 0.0$ Equation 12

$SS_{obs\_coa/model\_coa} = SO_4 + Cl$ Equation 13

IN_{model_coa} = Primary PM + SOIL Equation 14

After the data fusion, this dataset is apportioned into the three modes based on surface $PM_{2.5}$ and PM_{10} measurements from IMPROVE. These three modes are Aitken (0.01 – 0.1µm), accumulation (0.1 – 2.5µm) and coarse (2.5 – 40µm). In other words, we approximate a fraction from the total masses near surface for each mode then use the same ratio for each layer. There is an uncertainty in this approximation method due to the limited of observations.

By utilizing the lognormal distribution (Equation 15) (Binkowski 1999) with the total mass of each mode, the geometric mean diameter and geometric standard deviation for each mode can be estimated. The log-normal size distribution of aerosol number is represented as,

$$n(lnD) = \frac{N}{\sqrt{2\pi}\, ln\sigma_g} exp\left[-0.5\left(\frac{ln\frac{D}{D_g}}{ln\sigma_g}\right)^2\right] \quad \text{Equation 2}$$

where N is the particle number concentration within the mode, D is the particle diameter, and D_g and σ_g are the geometric mean diameter and geometric standard deviation, respectively, of the mode.

Since the aerosol component of SCM is same as that in the coupled model, extracting input data (i.e. size resolved composition profiles) from coupled model requires minimal processing. The coupled model has the same categories of size and composition as well as vertical layer structure. The profiles are extracted directly from the grid cells where the supersites are located. Note that the elevations for the supersites are different (see Figure 1).

The computation of SCM extinction and SSA from the observations or coupled model input uses the chemical speciation defined in Equations 2 through 14. This speciation is used in the optical calculation as follows. The speciated masses are converted into volume using the density of each lumped species. The volume weighted RIs are calculated from observations or coupled model inputs as appropriate. For the coarse mode, EC is assumed to be absent, and therefore only BHMIE is used to calculate scattering and absorption. For the Aitken and accumulation modes where EC is present, BHCOAT is used. That is, the particles are assumed to have a core composed of EC with a shell coating of other species.

4. Results

Analysis of SCM results for two cases during the CARES field study are presented in this section – these were on June 14 and June 24, 2010, when measurements from aircraft spirals were available in vicinity of the surface supersites.

4.1 Study Cases

Case 1 (June 14, 2010, Local time)

As shown in Figure 3 (a), the vertical profile between UTC 17:18 to UTC 17:24 was selected to be used in the SCM test. The horizontal spatial extent of the flight route conducted by the G-1 (see Figure 3 b) shows that this ascending spiral was between the two supersites.

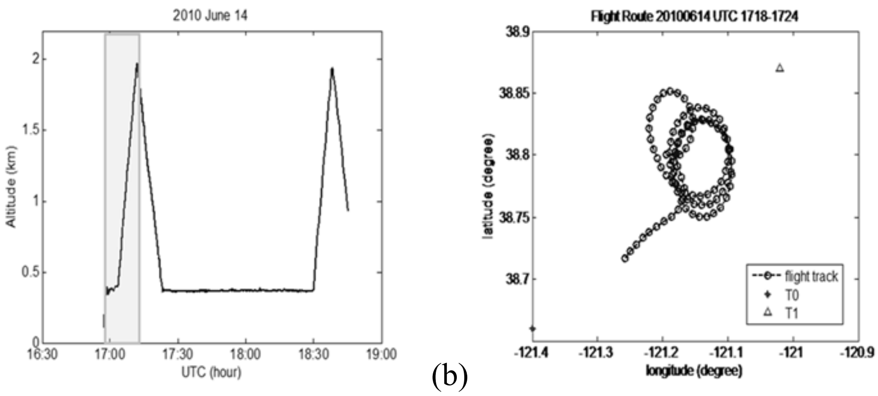

(a) (b)

Figure 3: (a) Vertical profile of G1 flight on June 14, 2010, (b) and selected flight path (in green box) for Case 1.

First, we examine the aerosol extinction estimated from the SCM using size resolved composition profiles estimated from the observation as input (i.e. identified as “obs input”) and extracted from coupled WRF-CMAQ simulations at locations of supersites T0 and T1 (i.e. identified as “T0 and T1 model input”) compared with the direct aerosol extinction measurements (i.e. labeled as “neph + psap” which is representing the combined contribution of scattering from nephelometer and absorption from PSAP). In order to have optimal aerosol extinction matching, we also extract the aerosol extinction from the coupled model output based on the G1 flight route (e.g. spatially and temporally) which is labeled as “G1 model” in Figure 4. Note that the aerosol extinction estimated using coupled model input and G1 route included the IN (see equation 5, 10, 14) contribution.

As shown in Figure 4 (a-c), the extinctions for wavelengths (450nm, 550nm and 700nm) estimated from SCM based on the observation input profiles of aerosol size and composition (“obs input”) match well with the direct observed extinction profiles (“neph + psap”). However, the extinctions estimated by the SCM based on the coupled model input profiles at both supersites T0 and T1 are lower than the observed extinction. With the purpose of matching the extinction properly, we extracted the extinction based on G1 flight path temporally and spatially. The “G1 model” extinction estimate looks more like those estimated extinction extracted at T0 and T1 sites than the extinction derived from the observation input profiles. This is indicative of a systematic low bias in aerosol loading predicted by the model in the region of this sampling.

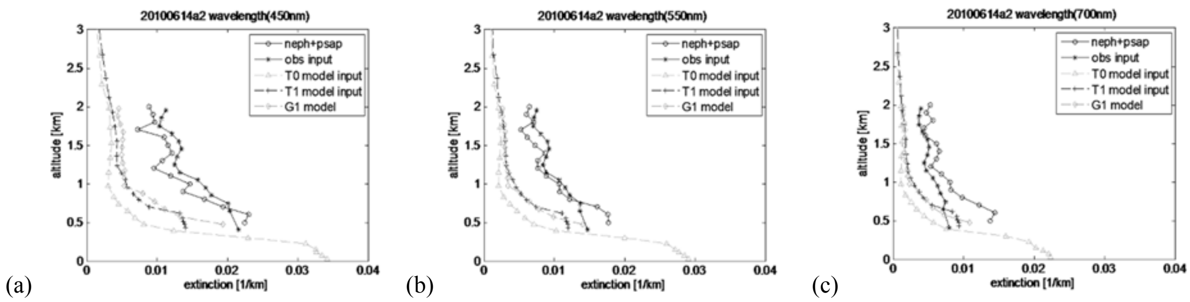

Figure 4: Vertical profiles for extinction at wavelengths (a) 450 nm, (b) 550 nm and (c) 700 nm on June 14, 2010. “neph + psap” means direct measurement made on the aircraft, “obs input” means output from SCM derived from observation input profiles while “T0 / T1 model input” mean output from SCM derived from coupled model input profiles. “G1 model” means coupled model direct output extracted based on G1 flight route.

A comparison of the estimated SSA and AOD from different tests is illustrated in Figure 5 (a) and (b), respectively. The mean SSAs between 0.5 km and 2 km are listed in Table 2. As shown in Table 2, the SSA from SCM (both observation and coupled model size resolved composition profiles) and direct-coupled model output are lower than the observations. Even the SCM results using observed inputs does not agree well with observed SSA, which suggests that further development of the SSA calculation is needed. For instance, external mixing is not considered in the WRF-CMAQ model while the BHCOAT can potentially enhance absorption extinction which may lead to underpredicted SSA. Significant vertical variation in the observed SSA is apparent in Figure 5(a), and it should be noted that the observed SSA is an estimate (i.e. retrieved parameter) based on the aerosol extinction measurements at 550 nm wavelength with some assumptions. In Figure 5 (b), the AOD at any altitude is estimated as the integral of the extinction between that altitude and 2km. For the AOD, only the observation input case is similar to the observed value while the other cases are much lower.

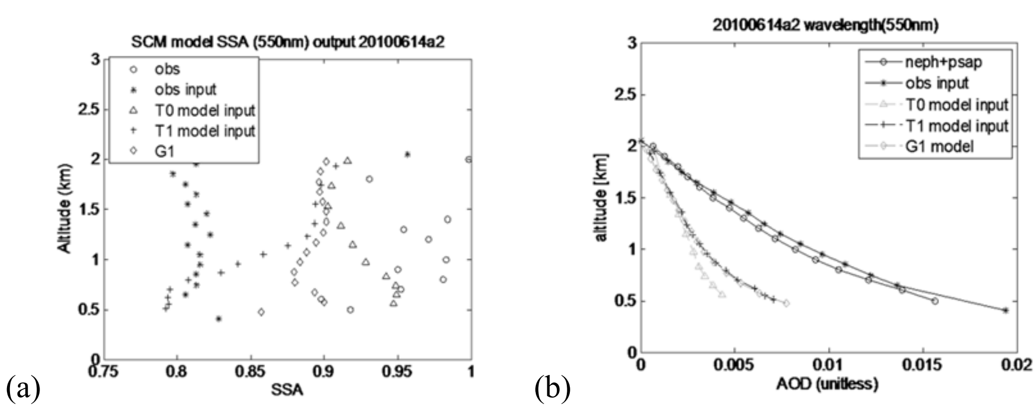

Figure 5: (a) Vertical profiles for SSA at 550 nm wavelength between 0.5 to 2 km, (b) 550 nm AOD calculated between 0.5 and 2 km on June 14, 2010. “obs” means observation, “obs input” means output from SCM derived from observation input profiles while “T0 / T1 model input”

mean output from SCM derived from coupled model input profiles. “G1 model” means direct coupled model output extracted based on G1 flight route.

Table 2 Calculated mean SSA and AOD at 550 nm wavelength between 0.5 to 2 km for Case 1.

	SSA	AOD_0.5km
obs	0.96	0.0157
scm_obs	0.82	0.0194
scm_t0	0.93	0.0043
scm_t1	0.85	0.0071
G1 model	0.89	0.0063

After assessing the extinctions, we compare the observed RH, temperature and species concentrations with model data extracted over the T0 and T1 supersites to gain further insight on the effects of these variables on the estimated aerosol optical characteristics. Since we estimated the aerosol water content based on RH in conjunction with ISORROPIA, it is important to assess consistency of the modeled and observed RH profile. As shown in Figure 6, the RH and temperature from the coupled model are within the range of the observation.

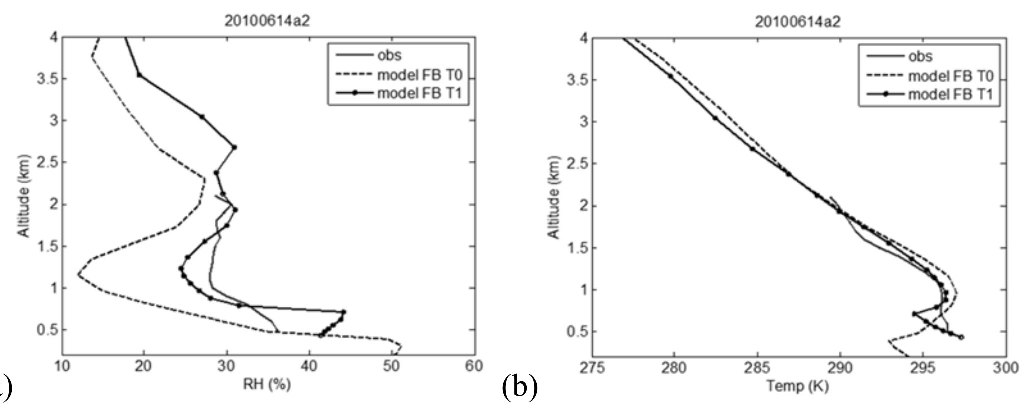

(a) (b)

Figure 6: (a) Vertical profiles of RH and (b) vertical profiles of temperature on June 14, 2010. “obs” means observation while “model FB T0 / T1” mean coupled model.

Next, we compare the species concentrations (i.e. water content, WS, EC and SS) in three size modes. Figure 7 (a-c) shows the water content obtained from the coupled model at T0 and T1. The water content in the accumulation and coarse modes are within the observation range above 1 km while the water content in Aitken mode is lower than the observation at all altitudes. Note that water content of accumulation and coarse modes are over predicted below 1 km in the coupled model. On the other hand, the WS profiles obtained from coupled model at T0 and T1 for Aitken and accumulation modes are much lower than the observed profiles (see Figure 8 (a) and (b)). Also, note that in the current implementation of the WRF-CMAQ system, carbonaceous aerosols (both primary and secondary) are considered to be constituents of the insoluble component in the accumulation mode. The relative partitioning of the various OC constituents into the soluble and insoluble fractions is highly uncertain and assumptions invoked can influence the estimated RI and thus the extinction and AOD.

In the initial comparisons the water soluble OC is not considered in the accumulation mode of WS of the coupled model while it was included in the observation input profile to run the SCM. The solid black line without marker in Figure 8 (b) shows the OC mass ("oc obs") is fairly large. Even though IN was included in the coupled model input, the extinction of three wavelengths was still lower than observation. This indicates that species included in the WS_{model} are insufficient. A recent study by Cahill et al (2012) demonstrates that the aerosol composition varies greatly in California, with nitrate and soot being dominant species in southern California while sulfate and OC dominate in northern California. Therefore, it is important to have precise representation of varieties aerosol species (e.g. primary and secondary) regionally.

The original design for the WRF-CMAQ model treats OC as IN. However, some fraction of OC is known to be water soluble [Timonen et al., 2012]. Also be aware the current version of WRF-CMAQ model does not include hygroscopic properties for water soluble OC and the RI and density for each lumped species may need to be redefined. Thus one of the potential improvements is to make the necessary changes in WRF-CMAQ model to account for water soluble OC. This work is ongoing for WRF-CMAQ model development.

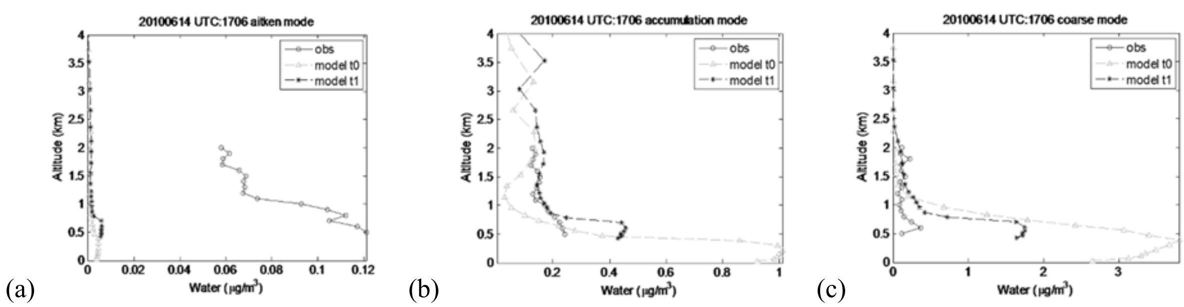

Figure 7: Vertical profiles of water content for (a) Aitken, (b) accumulation and (c) coarse modes on June 14, 2010. "obs" means observation while "model t0 / t1" mean coupled model.

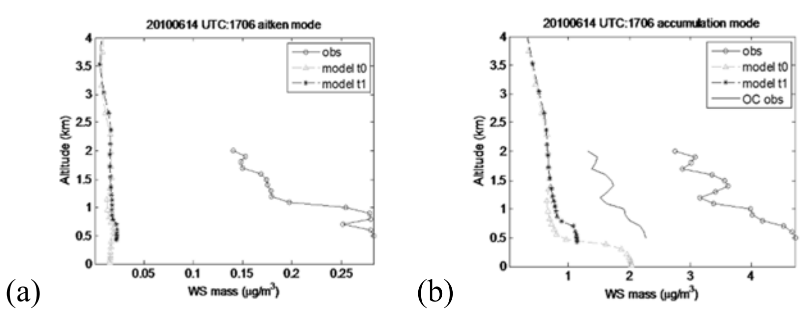

Figure 8: Vertical profiles of water soluble for (a) aitken and (b) accumulation modes on June 14, 2010. "obs" means observation while "model t0 / t1" mean coupled model.

For EC (see Figure 9), the coupled model profiles of concentration in the accumulation mode at T0 and T1 are within the range of the observations, but they are low in the Aitken mode, which should not make a significant impact on extinction as the observed EC is also low. Note that, in the coupled WRF-CMAQ model, WS and EC are not considered in coarse mode while SS is neglected in the Aitken mode, since the relative contributions of these constituents in these modes is negligible. Because of the low observed EC concentration, it is difficult to assess the absorption calculation in the model effectively in this study. Figure 10 illustrates that SS profiles of coarse mode obtained from the coupled model at T0 and T1 are in the range of the observation but very low in the accumulation mode. This finding indicates that the amount of SS in accumulation mode of model is underestimated and can play a role in the underestimation of the modeled extinction.

Lastly, IN vertical profiles from the coupled model are presented in Figure 11. As mentioned before, comparable measurements of the IN constituent sum are not available. In order to see the effect of IN in the SCM test, we compare in Figure 12 the aerosol extinction profiles at the three wavelengths for both supersites using coupled model input that contains all species (i.e. WS, SS, EC, IN and water) and another one that contains all species except IN (i.e. WS, SS, EC and water). As shown in these comparisons, the modeled IN only makes an insignificant contribution below 1 km and has almost no effect above it. Furthermore, according to Equation 5, 10 and 14, IN is represented by both primary and secondary organic and other species, and these definitions may need to be re-examined as some of the species should be considered as WS or maybe as new categories in the model. Furthermore, this ambiguous category may not have the right density and RI for the appropriate optical calculation which can affect the extinction contribution. Again, this finding shows that additional species such as water soluble OC need to be integrated in the coupled model.

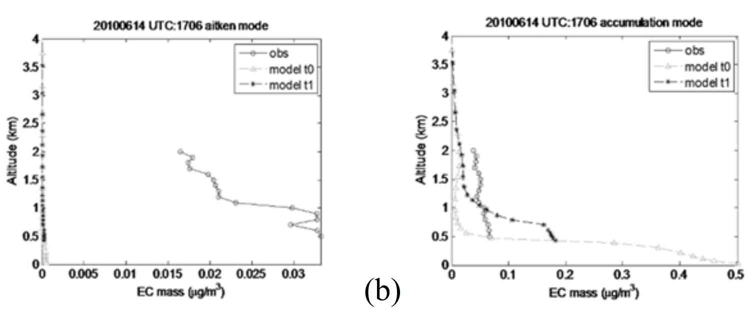

(a) (b)

Figure 9: Vertical profiles of element carbon for (a) aitken and (b) accumulation modes on June 14, 2010. “obs” means observation while “model t0 / t1” mean coupled model.

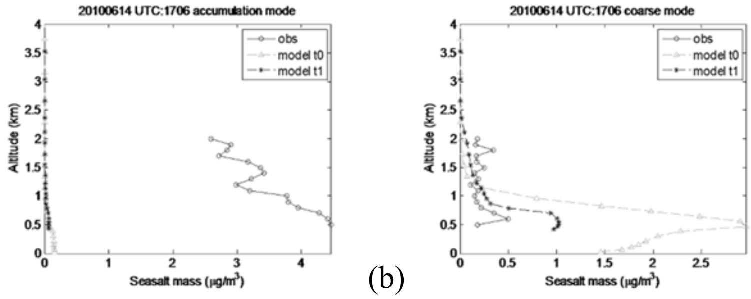

(a) (b)

Figure 10: Vertical profiles of sea-salt for (a) accumulation and (b) coarse modes on June 14, 2010. “obs” means observation while “model t0 / t1” mean coupled model.

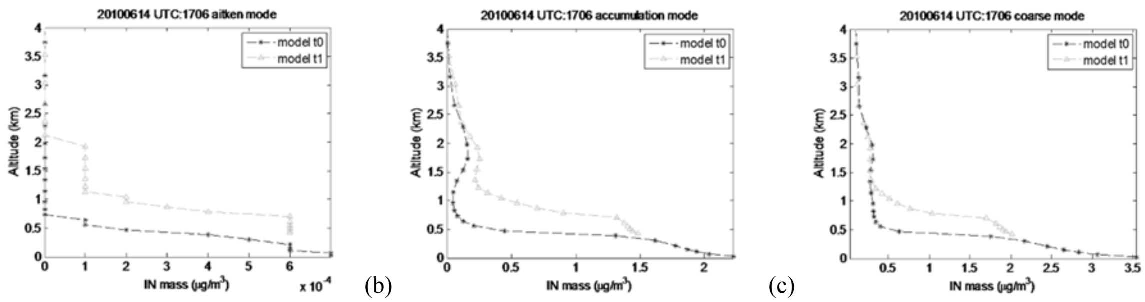

(a) (b) (c)

Figure 11: Vertical profiles of insoluble for (a) Aitken, (b) accumulation and (c) coarse on June 14, 2010. Note that observation “obs” was not available in this group and model t0 / t1” mean coupled model.

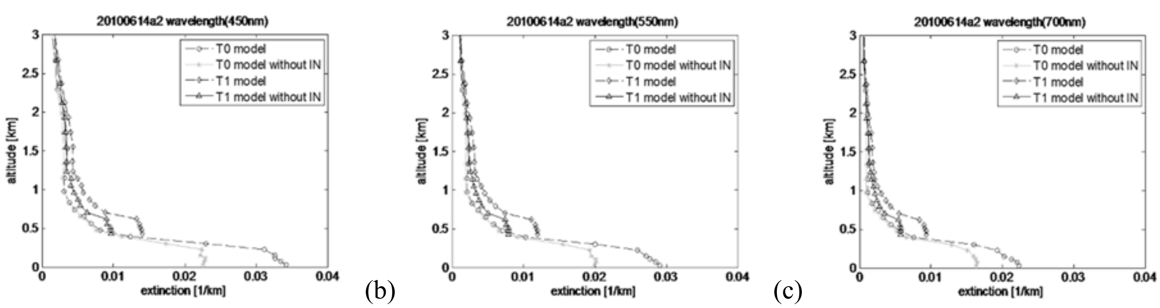

(a) (b) (c)

Figure 12: Vertical profiles for extinction at wavelengths (a) 450 nm, (b) 550 nm and (c) 700 nm on June 14, 2010. “T0 / T1 model” mean output from SCM derived from coupled model input profiles which included WS, SS, EC, IN and water. “T0 / T1 model without IN” mean output from SCM derived from coupled model input profiles which included WS, SS, EC and water only.

Case 2 (June 24, 2010, Local time)

The vertical profile between UTC 01:00 to UTC 01:12 on June 25, 2010 was used in the second case study (see Figure 13 (a)) and the flight path is shown in Figure 13 (b).

(a) 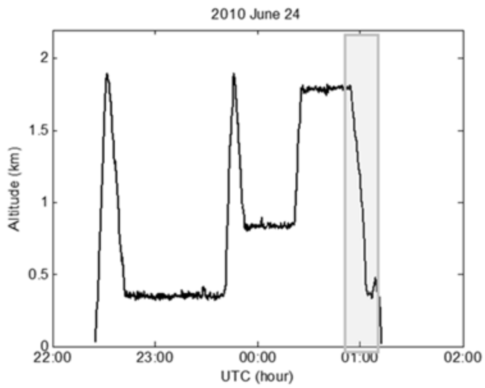

(b) 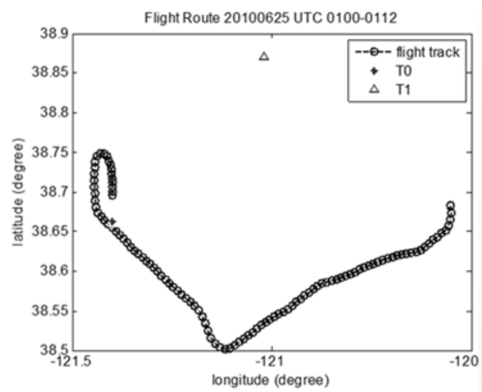

Figure 13: (a) Vertical profile of flight G1 on June 24, 2010, (b) and selected flight path (in green box) for Case 2.

In contrast to Case 1, as illustrated in Figure 14 (a-c), for this flight segment the extinction profiles extracted from the coupled model match the direct observations more closely as well as the observation input derived SCM extinction profiles. Also, the extinctions based on G1 flight route are extracted for comparison. They match reasonably well also for the three wavelengths.

When comparing the SSA in Figure 15, the SSA derived from the model inputs shows more variability (i.e. monotonically increases with height) than the SSA derived from the observation input (more constant with height). This may be related to the excessive decrease with height of absorbing species such as EC in the model results (see Figure 19), although the EC concentration is quite low for this case. Even though the observation input derived SSA is similar with the observed SSA, it is still underestimated. Note that, this case is not a particularly good test of SSA calculations because of the very low concentrations of observed EC. The AOD computed from the observed input profile and coupled model direct output (based on G1 route) is almost equivalent to the observation. In this case, the close match in the modeled and measured extinction profiles leads to slightly better agreement between the corresponding SSAs as compared to those in Case 1. However, these significant uncertainties in the SSA computations in the current WRF-CMAQ model related to mixing state, hygroscopic effect, RI and density for organic species that need to be determined and quantified.

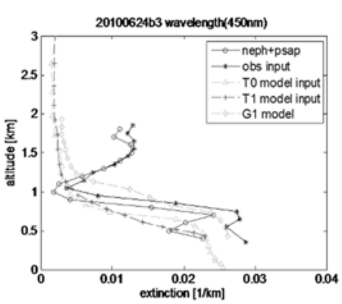

(a)
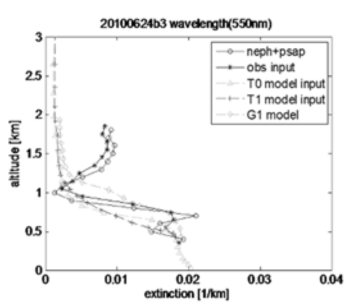

(b)
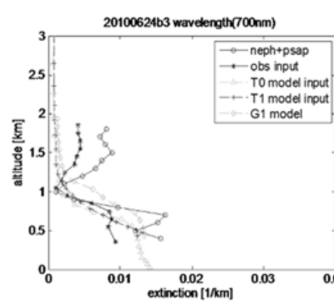

(c)

Figure 14: Vertical profiles for extinction at wavelengths (a) 450 nm, (b) 550 nm and (c) 700 nm on June 24, 2010. “neph + psap” means direct measurement made in the aircraft, “obs input” means output from SCM derived from observation input profiles while “T0 / T1 model input” mean

output from SCM derived from coupled model input profiles. “G1 model” means direct coupled model output extracted based o G1 flight route.

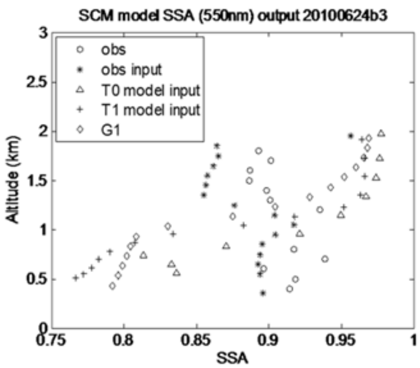

(a)

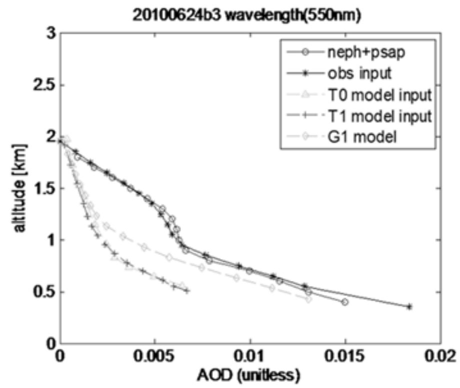

(b)

Figure 15: (a) Vertical profiles for SSA at 550 nm wavelength between 0.5 km and 2 km. (b) 550 nm AOD calculated between 0.5 and 2 km on June 24, 2010. “obs” means observation, “obs input” means output from SCM derived from observation input profiles while “T0 / T1 model input” mean output from SCM derived from coupled model input profiles. “G1 model” means direct coupled model output extracted based on G1 flight route.

Table 3 Calculated mean SSA and AOD at 550 nm wavelength between 0.5 km to 2 km for Case 2.

	SSA	AOD_0.5km
obs	0.91	0.0150
scm_obs	0.89	0.0183
scm_t0	0.91	0.0064
scm_t1	0.87	0.0067
G1 model	0.89	0.0112

The RH and temperature comparisons, presented in Figure 16 (a-b), show that the RH and temperature profiles from the coupled model match the observations well below 2 km. RH estimated from the coupled model increases at T0 and T1 above 1.3 and 2.2 km, respectively. The observations from the aircraft similarly show increasing RH above ~1 km though the modeled RH cannot be verified above 2 km, due to lack of measurements. Moreover, the species mass comparisons in this case study demonstrate a different scenario compared to Case 1. As shown in Figure 17, the water content from the coupled model does not well match with observation profiles except near the top of the aircraft profile for accumulation and coarse modes. Also, it was under predicted in Aitken mode and over predicted in accumulation and coarse modes below 1.5 km. The WS mass profiles show agreement between the coupled model and observations in Aitken and accumulation modes (see Figure 18) only for a thin layer at about 1 km with underestimations both above and below. In this case study, only a small amount of OC mass present (see the solid black line without marker in Figure 18 (b)).

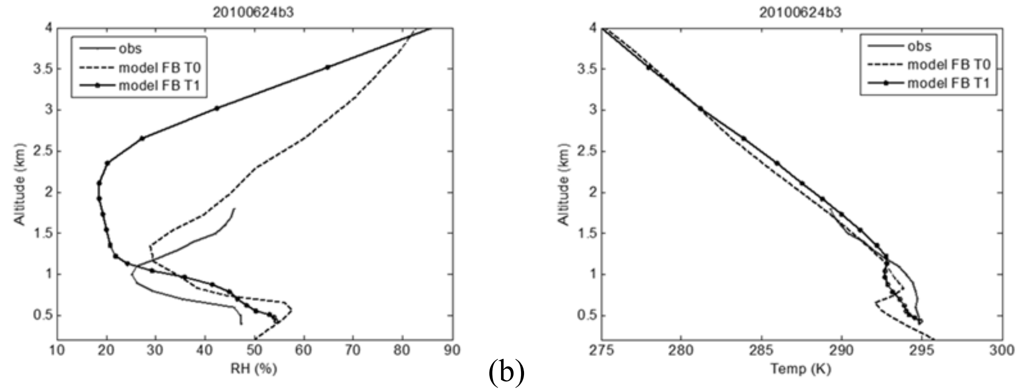

(a) (b)

Figure 16: (a) Vertical profiles of RH and (b) vertical profiles of temperature on June 24, 2010. “obs” means observation while “model FB T0 / T1” mean coupled model.

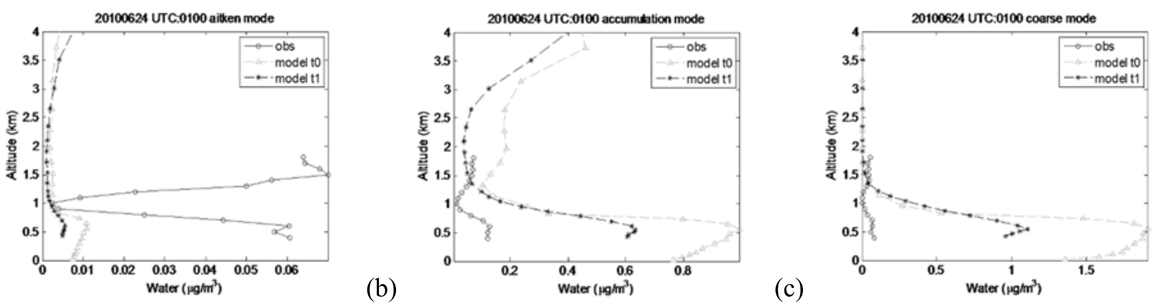

(a) (b) (c)

Figure 17: Vertical profiles of water content for (a) Aitken, (b) accumulation and (c) coarse modes on June 24, 2010. “obs” means observation while “model t0 / t1” mean coupled model.

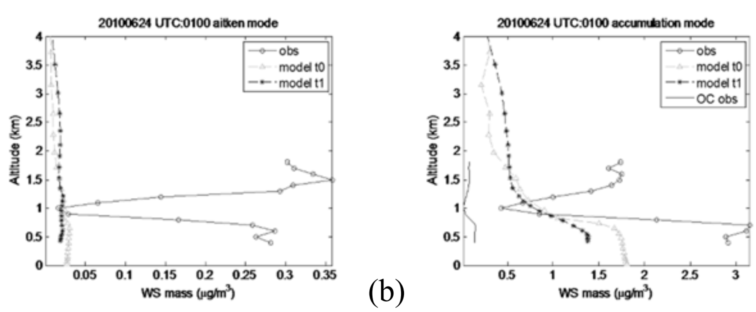

(a) (b)

Figure 18: Vertical profiles of water soluble for (a) Aitken and (b) accumulation modes on June 24, 2010. “obs” means observation while “model t0 / t1” mean coupled model.

The EC in the Aitken mode and SS in the accumulation mode from the coupled model are less than the observation while the SS in the coarse mode are more similar to the observation (see Figure 19 and 20). The EC in the accumulation mode is between the observation around 1 km but overestimated below 1 km. For IN of the three modes, they behave similar as Case 1 which is low above 1 km and a small contribution below 1 km (see Figure 21 and 22)

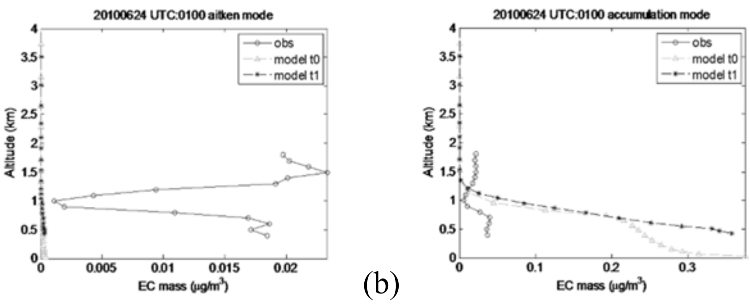

(a) (b)

Figure 19: Vertical profiles of element carbon for (a) Aitken and (b) accumulation modes on June 24, 2010. “obs” means observation while “model t0 / t1” mean coupled model.

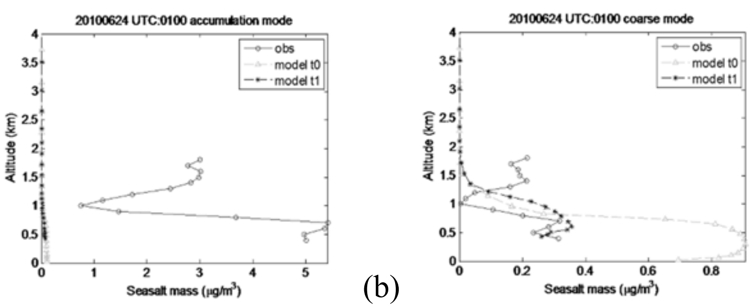

(a) (b)

Figure 20: Vertical profiles of sea-salt for (a) accumulation and (b) coarse modes on June 24, 2010. “obs” means observation while “model t0 / t1” mean coupled model.

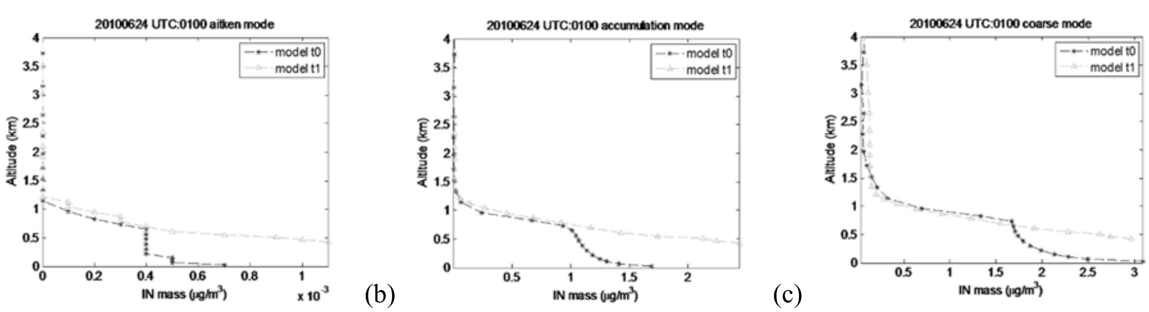

(a) (b) (c)

Figure 21: Vertical profiles of insoluble for (a) Aitken, (b) accumulation and (c) coarse on June 24, 2010. Note that observation “obs” was not available in this group and model t0 / t1” mean coupled model.

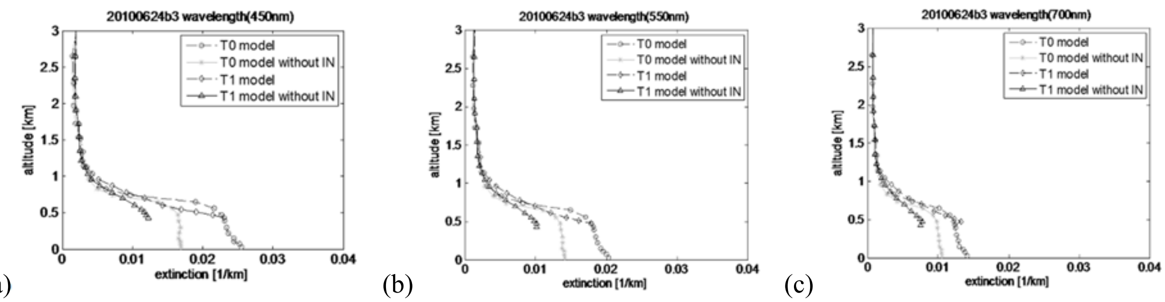

(a) (b) (c)

Figure 22: Vertical profiles for extinction at wavelengths (a) 450 nm, (b) 550 nm and (c) 700 nm on June 24, 2010. "T0 / T1 model" mean output from SCM derived from coupled model input profiles which included WS, SS, EC, IN and water. "T0 / T1 model without IN" mean output from SCM derived from coupled model input profiles which included WS, SS, EC and water only.

In this case, the agreement between modeled and observed species mass is better than Case 1 and consequently leads to the noted better performance for aerosol extinction. In the observations, an aloft layer of elevated particulate matter is noted (and is not captured by the model), presumably representative of the previous day residual layer. Further exploration of this feature and its contribution to the observed AOD can be an interesting element for future studies. Improvements in representation of SS emissions could potentially lead to improved representation of aerosol composition (especially in the accumulation mode) and possibly much better agreement in the estimated extinction values.

4.2 Discussion

Numerical closure experiments using detailed and concurrent measurements of aerosol size, composition, and optical properties are performed with a SCM based on the aerosol optics algorithms of the coupled WRF-CMAQ model to evaluate the robustness of the model in estimating aerosol optical characteristics and consequently their modeled radiative effects. When observations of aerosol mass and size are used to constrain the volume weighted estimation of the RI and subsequent calculation of aerosol optical properties, the SCM modeled values of extinction and AOD match well the corresponding observed values. For the two cases examined here, the WRF-CMAQ derived extinction values were underestimated compared to observations, and this underestimation was found to arise from underestimation of specific aerosol constituents such as OC, low SS concentration in the accumulation mode and uncertainties in characterizing the water soluble potion of the OC leading to poor representation of RI of organic aerosol. Moreover, the current version WRF-CMAQ does not consider hygroscopic effects of water soluble OC and external mixing. The omitted effects and incomplete representation of mixing state can play an important role in the apportionment of extinction [Cappa et al., 2012, Hu et al., 2010, Malm and Kreidenweis, 1998 and Tang, 2012].

In particular, Case 1 shows a significant amount of OC in the observation. When the SCM is rerun with the coupled model extracted input at T0, T1, and following the G1 flight path for both cases but with observed OC added to the WS portion of the aerosol, the estimated extinction values agreed much better with observations compared to the original Case 1 configuration. The AOD at 0.5 km altitude (0.0129 at T0 and 0.0078 at T1) also increased for Case 1 compared to the original AOD (0.0060 at T0 and 0.0044 at T1) but with no major change in SSA. For Case 2, the performance of extinction is similar to the original test result since only a small amount of OC was present in the observation. Therefore, improving the representation of OC mass as well as a better characterization of the water soluble portion can improve the performance of the aerosol module of the coupled model. In addition, the RI and density of each species need to be examined and updated accordingly. For instance, Li et al (2014) stated that the RIs of the secondary organic aerosols vary dramatically when the NO_x concentration changes. Currently, the WRF-CMAQ model uses the OPAC values for the RI of WS and IN aerosol components. In particular, the RI for WS are based upon inorganic species especially sulfates and nitrates.

Another possible solution is to increase the SS emission near the coastal regions especially in the accumulation mode. As shown by Evgueni et al (2012) there was a significant contribution of coarse mode aerosol in central California to aerosol radiative forcing. For instance, removal of large particles in the evaluation leads to an increase in SSA. Consequently, this can increase the calculated cooling effect of aerosols, up to 45% and 30% for $PM_{1.0}$ and $PM_{2.5}$ cases, respectively. Moreover, the cutoff point between the accumulation and coarse modes in the model may need to be reexamined. When constructing the size resolved composition profiles, the sensitivity tests (result is not presented here) indicated part of the accumulation mode masses maybe incorrectly partitioned into coarse mode. For example, Kelly et al (2011) stated the accumulation mode diameters and widths were over predicted in the CMAQ wintertime simulation in California.

Last but not least, a series of sensitivity tests (e.g. RI, density, mixing state, water soluble organic treatment and hygroscopic effect) for SSA needs to be conducted to improve its performance. These studies are under way and will be reported in future contributions.

5. Conclusions

The SCM results using measured aerosol inputs show that the aerosol optics calculations employed in the coupled WRF-CMAQ model are fairly accurate, in particular for estimating scattering extinction. In conclusion, the extinction from the model is always lower than the observation which may be due to the missing species or insufficient masses such as water soluble OC and SS, emission source strengths, poor representation of IN, inaccurate representation of RI, omitted hygroscopic effect on water soluble OC and incomplete mixing state representation but not owing to the computation of aerosol optics. In general, the scattering calculation in the model is working well but the absorption calculation needs to be further improved.

Acknowledgements

This research was performed while Chuen-Meei Gan held a National Research Council Research Associateship Award at US EPA. The research presented in this study was supported through an interagency agreement between the US Department of Energy (funding IA DE-SC0003782) and the US Environmental Protection Agency (funding IA RW-89-9233260). It has been subject to the US EPA's administrative review and approved for publication. We would like to thank Kirk Baker and James Kelly from OAQPS of US EPA for their support and assistance in obtaining the emission dataset. We also thank the numerous CARES investigators for providing field campaign data used in this study. We also appreciate the comments of two reviewers that have significantly improved this paper.

References

Bahreini, R., Ervens, B., Middlebrook, A. M., Warneke, C., deGouw, J. A., DeCarlo, P. F., Jimenez, J. L., Brock, C. A., Neuman, J. A., Ryerson, T. B., Stark, H., Atlas, E., Brioude, J., Fried, A., Holloway, J. S., Peischl, J., Richter, D., Walega, J., Weibring, P., Wollny, A. G., and Fehsenfeld, F. C.: Organic aerosol formation in urban and industrial plumes near Houston and Dallas, Texas, J. Geophys. Res., 114, D00F16, doi:10.1029/2008JD011493, 2009.

Bani Shahabadi, M., and Huang, Y.: Logarithmic radiative effect of water vapor and spectral kernels, J. Geophys. Res. Atmos., 119, *doi:*10.1002/2014JD021623, 2014

Baumgardner, D., Jonsson, H., Dawson, W., O'Connor, D. and Newton, R.: The cloud, aerosol and precipitation spectrometer: a new instrument for cloud investigations, Armospheric Research 59-60(2001)251-264, DOI: 10.1016/S0169-8095(01)00119-3, 2001.

Bond,T.C., Anderson, T.L., Campbell, D.,"Calibration and intercomparison of filter-based measurements of visible light absorption by aerosols," Aerosol Science and Technology, vol. 30, pp582-600, 1999.

Binkowski, F. S.: Aerosols in models-3 CMAQ, in Science Algorithms of EPA Models-3 Community Multiscale Air Quality (CMAQ) Modeling System, chap. 10, EPA/600/R-99/030, Off. Of Res. And Dev., U.S. Environ. Prot. Agency, Washington, D.C., 1999.

Binkowski, F. S., and Rosselle, S. J.: Models-3 Community Multiscale Air Quality (CMAQ) model aerosol component, 1. Model description, J. Geophys. Res., 108(D6), 4183, doi:10.1029/2001JD001409, 2003.

Bohren, C. F. and Huffman, D. R.: Absorption and scattering of light by small particles, New York : Wiley, 530 p., ISBN 0-471-29340-7, ISBN 978-0-471-29340-8 (second edition), 1998.

Cahill, J. F., Suski, K., Seinfeld, J. H., Zaveri, R. A., and Prather, K. A.: The mixing state of carbonaceous aerosol particles in northern and southern California measured during CARES and CalNex 2010, Atmos. Chem. Phys., 12, 10989-11002, doi:10.5194/acp-12-10989-2012, 2012.

Cai, Y., Montague, D., Mooiweer-Bryan, W. and Deshler, T.: Performance characteristics of the ultra high sensitivity aerosol spectrometer for particles between 55 and 800 nm: Laboratory and field studies, Journal of Aerosol Science 39 759-769, doi:10.1016/j.jaerosci.2008.04.007, 2008.

Canagaratna M. R., Jayne, J. T., Jimenez, J. L., Allan, J. D., Alfarra, M. R., Zhang, Q., Onasch, T. B., Drewnick, F., Coe, H., Middlebrook, A., Delia, A., Williams, L. R., Trimborn, A. M., Northway, M. J., DeCarlo, P. F., Kolb, C. E., Davidovits, P., and Worsnop, D. R.: Chemical and microphysical characterization of ambient aerosols with the aerodyne aerosol mass spectrometer, Mass Spectrom Rev., 62, 185–222, doi:10.1002/mas.20115, 2007.

Cappa et al.: Radiative Absorption Enhancements Due to the Mixing State of Atmospheric Black Carbon, 337 (6098): 1078-108, *OI:* 10.1126/science.122344, 2012.

Chen, Y. and Bond, T. C.: Light absorption by organic carbon from wood combustion, Atmos. Chem. Phys., 10, 1773-1787, doi:10.5194/acp-10-1773-2010, 2010.

Clough, S. A., Iacono, M. J. and Moncet, J.-L.: Line-by-line calculations of atmospheric fluxes and cooling rates: Application to water vapor, J. Geophys. Res., 97(D14), 15761–15785, *doi:*10.1029/92JD01419, 1992.

Fast, J.D., Gustafson Jr., W.I. , Chapman, E.G., Easter, R.C., Rishel, J. , Zaveri, R.A., Grell, G. and Barth, M.: The Aerosol Modeling Testbed: A community tool to objectively evaluate aerosol process modules. Bull. Amer. Meteor. Soc., 92, 343-360, 2011.

Fast, J.D., Shrivastava, M., Velu, V. and Song, C.: Aerosol Modeling Testbed: CARES Field Campaign Data in the Analysis Toolkit Format, DOE/SC-ARM/TR-XXX. version 1.0., June 5, 2012.

Fast, J. D., Allan, J., Bahreini, R., Craven, J., Emmons, L., Ferrare, R., Hayes, P. L., Hodzic, A., Holloway, J., Hostetler, C., Jimenez, J. L., Jonsson, H., Liu, S., Liu, Y., Metcalf, A., Middlebrook, A., Nowak, J., Pekour, M., Perring, A., Russell, L., Sedlacek, A., Seinfeld, J., Setyan, A., Shilling, J., Shrivastava, M., Springston, S., Song, C., Subramanian, R., Taylor, J. W., Vinoj, V., Yang, Q., Zaveri, R. A., and Zhang, Q.: Modeling regional aerosol and aerosol precursor variability over California and its sensitivity to emissions and long-range transport during the 2010 CalNex and CARES campaigns, Atmos. Chem. Phys., 14, 10013-10060, doi:10.5194/acp-14-10013-2014, 2014.

Hess, M., Koepke, P. and Schult, I.: Optical Properties of Aerosols and Clouds: The Software Package OPAC. Bull. Amer. Meteor. Soc., **79**, 831–844. doi: http://dx.doi.org/10.1175/1520-0477(1998)079<0831:OPOAAC>2.0.CO;2, 1998.

Hu, D., Qiao, L., Chen, J., Ye, X., Yang, X., Cheng, T. and Fang, W.: Hygroscopicity of Inorganic Aerosols: Size and Relative Humidity Effects on the Growth Factor. Aerosol and Air Quality Research, 10: 255-264, doi: 10.4209/aaqr.2009.12.0076, 2010.

Kassianov, E., Pekour, M. *and* Barnard, J.: Aerosols in central California: Unexpectedly large contribution of coarse mode to aerosol radiative forcing, Geophys. Res. Lett., 39, *L20806, doi:*10.1029/2012GL053469, 2012.

Kelly, J. T., Cai, C., Avise, J. and Kaduwela, A.: Simulating particle size distributions over California and impact on lung deposition fraction, Aerosol Sci. Technol., 45(2), 148–162, 2011.

Kelly, J. T., et al.: Fine-scale simulation of ammonium and nitrate over the South Coast Air Basin and San Joaquin Valley of California during CalNex-2010, J. Geophys. Res. Atmos., 119, 3600–3614, *doi:*10.1002/2013JD021290, 2014.

Kulkarni,P.,and Wang, J. (2006a). New fast integrated mobility spectrometer for real-time measurement of aerosol size distribution—I: Concept and theory. *Journal of Aerosol Science*, *37*, 1303–1325.

Kulkarni,P.,and Wang,J. (2006b). New fast integrated mobility spectrometer for real-time measurement of aerosol size distribution: II. Design, calibration, and performance characterization. *Journal of Aerosol Science*, *37*, 1326–1339.

Laborde, M., Schnaiter, M., Linke, C., Saathoff, H., Naumann, K. H., Möhler, O., Berlenz, S., Wagner, U., Taylor, J. W., Liu, D., Flynn, M., Allan, J. D., Coe, H., Heimerl, K., Dahlkötter, F., Weinzierl, B., Wollny, A. G., Zanatta, M., Cozic, J., Laj, P., Hitzenberger, R., Schwarz, J. P., and Gysel, M.: Single Particle Soot Photometer intercomparison at the AIDA chamber, Atmos. Meas. Tech., 5, 3077–3097, doi:10.5194/amt-5-3077-2012, 2012.

Langridge, J. M., Lack, D., Brock, C. A., Bahreini, R., Middlebrook, A. M., Neuman, J. A., Nowak, J. B., Perring, A. E., Schwarz, J. P., Spackman, J. R., Holloway, J. S., Pollack, I. B., Ryerson, T. B., Roberts, J. M., Warneke, C., de Gouw, J. A., Trainer, M. K., and Murphy, D. M.: Evolution of aerosol properties impacting visibility and direct climate forcing in an ammonia-rich urban environment, J. Geophys. Res., 117, D00V11, doi:10.1029/2011JD017116, 2012.

Li, K., Wang, W.G., Ge, M.F., Li, J.J. and Wang, D.: Optical properties of secondary organic aerosols generated by photooxidation of aromatic hydrocarbons. Sci. Rep. 4, 4922; doi:10.1038/srep04922 (2014).

Malm, W. and Kreidenweis, S.: The effects of models of aerosol hygroscopicity on the apportionment of extinction. Atmos. Env. Vol. 31, Issue 13, 1965-1976, doi: 10.1016/S1352-2310(96)00355-X, 1997.

Massoli, P., Murphy, D. M., Lack, D. A., Baynard, T., Brock, C. A. and Lovejoy, E. R.: Uncertainty in Light Scattering Measurements by TSI Nephelometer: Results from Laboratory Studies and Implications for Ambient Measurements, Aerosol Science and Technology, 43:11, 1064-1074, DOI: 10.1080/02786820903156542

Mathur, R.: Estimating the impact of the 2004 Alaskan forest fires on episodic particulate matter pollution over the eastern United States through assimilation of satellite-derived aerosol optical depths in a regional air quality model, Geophysical Research, 113(D17), DOI: 10.1029/2007JD009767, 2008.

Mebust, M. R., Eder, B. K., Binkowski, F. S. and Roselle, S. J.: Models-3 Community Multiscale Air Quality (CMAQ) model aerosol component, 2, Model evaluation, J. Geophys. Res., 108(D6), 4184, doi:10.1029/2001JD001410, 2003.

Metcalf, A. R., Craven, J. S., Ensberg, J. J., Brioude, J., Angevine, W., Sorooshian, A., Duong, H. T., Jonsson, H. H., Flagan, R. C., and Seinfeld, J. H.: Black carbon aerosol over the Los Angeles Basin during CalNex, J. Geophys. Res., 117, D00V13, doi:10.1029/2011JD017255, 2012.

Michalsky, J. J., Anderson, G. P., Barnard, J., Delamere, J., Gueymard, C., Kato, S., Kiedron, P., McComiskey, A. and Ricchiazzi, P.: Shortwave radiative closure studies for clear skies during the Atmospheric Radiation Measurement 2003 Aerosol Intensive Observation Period, J. Geophys. Res., 111, *D14S90, doi:*10.1029/2005JD006341, 2006.

Middlebrook., A. M., Bahreini, R., Jimenez, J. L., and Canagaratna, M. R.: Evaluation of composition-dependent collection efficiencies for the Aerodyne Aerosol Mass Spectrometer using field data, Aerosol Sci. Tech., 46, 258–271, doi:10.1080/02786826.2011.620041, 2012.

Müller, T., Laborde, M., Kassell, G. and Wiedensohler. A.: Design and performance of a three-wavelength LED-based total scatter and backscatter integrating nephelometer, *Atmospheric Measurement Techniques* 4, no. 6 : 1291-1303, doi: 10.5194/amt-4-1291-2011.

Nenes A., Pandis S. N. and Pilinis C.: ISORROPIA: A new thermodynamic equilibrium model for multiphase multicomponent inorganic aerosols, Aquat. Geoch., 4, 123-152., 1998a.

Nenes A., Pilinis C., and Pandis S.N.: Continued Development and Testing of a New Thermodynamic Aerosol Module for Urban and Regional Air Quality Models, Atmos. Env., 33, 1553-1560, 1998b.

Roy et al: A comparison of CMAQ-based aerosol properties with IMPROVE, MODIS, and AERONET data, Journal of Geophysical Research, 112(D14), DOI: 10.1029/2006JD008085, 2007.

Schmid, B., et al.: How well do state-of-the-art techniques measuring the vertical profile of tropospheric aerosol extinction compare? J. Geophys. Res., 111, *D05S07, doi:*10.1029/2005JD005837, 2006.

Shilling, J. E., Zaveri, R. A., Fast, J. D., Kleinman, L., Alexander, M. L., Canagaratna, M. R., Fortner, E., Hubbe, J. M., Jayne, J. T., Sedlacek, A., Setyan, A., Springston, S., Worsnop, D. R., and Zhang, Q.: Enhanced SOA formation from mixed anthropogenic and biogenic emissions during the CARES campaign, Atmos. Chem. Phys., 13, 2091-2113, doi:10.5194/acp-13-2091-2013, 2013.

Setyan, A., Zhang, Q., Merkel, M., Knighton, W. B., Sun, Y., Song, C., Shilling, J. E., Onasch, T. B., Herndon, S. C., Worsnop, D. R., Fast, J. D., Zaveri, R. A., Berg, L. K., Wiedensohler, A., Flowers, B. A., Dubey, M. K., and Subramanian, R.: Characterization of submicron particles influenced by mixed biogenic and anthropogenic emissions using high-resolution aerosol mass spectrometry: results from CARES, Atmos. Chem. Phys., 12, 8131-8156, doi:10.5194/acp-12-8131-2012, 2012.

Tang, I. N.: Chemical and size effects of hygroscopic aerosols on light scattering coefficients, J. Geophys. Res., 101(D14), 19245–19250, *doi:*10.1029/96JD03003. 2012.

Timonen, H., et al.: Characteristics, sources and water-solubility of ambient sub-micron organic aerosol in spring time in Helsinki, Finland, Journal of Aerosol Science, http://dx.doi.org/10.1016/ j.jaerosci.2012.06.005, 2012.

vanWeele, M., et al.: From model intercomparison toward benchmark UV spectra for six real atmospheric cases, J. Geophys. Res., 105(D4), 4915–4925, *doi:*10.1029/1999JD901103, 2000.

Weber, R. J., D. Orsini, Y. Daun, Y-N. Lee, P. J. Klotz, and F. Brechtel. "A particle-into-liquid collector for rapid measurement of aerosol bulk chemical composition." *Aerosol Science & Technology* 35, no. 3 (2001): 718-727.

Wong, D. C., Pleim, J., Mathur, R., Binkowski, F., Otte, T., Gilliam, R., Pouliot, G., Xiu, A., Young, J. O., and Kang, D.: WRF-CMAQ two-way coupled system with aerosol feedback: software development and preliminary results, Geosci. Model Dev., 5, 299-312, doi:10.5194/gmd-5-299-2012, 2012.

Zaveri, R. A., Shaw, W. J., Cziczo, D. J., Schmid, B., Ferrare, R. A., Alexander, M. L., Alexandrov, M., Alvarez, R. J., Arnott, W. P., Atkinson, D. B., Baidar, S., Banta, R. M., Barnard, J. C., Beranek, J., Berg, L. K., Brechtel, F., Brewer, W. A., Cahill, J. F., Cairns, B., Cappa, C. D., Chand, D., China, S., Comstock, J. M., Dubey, M. K., Easter, R. C., Erickson, M. H., Fast, J. D., Floerchinger, C., Flowers, B. A., Fortner, E., Gaffney, J. S., Gilles, M. K., Gorkowski, K., Gustafson, W. I., Gyawali, M., Hair, J., Hardesty, R. M., Harworth, J. W., Herndon, S., Hiranuma, N., Hostetler, C., Hubbe, J. M., Jayne, J. T., Jeong, H., Jobson, B. T., Kassianov, E. I., Kleinman, L. I., Kluzek, C., Knighton, B., Kolesar, K. R., Kuang, C., Kubátová, A., Langford, A. O., Laskin, A., Laulainen, N., Marchbanks, R. D., Mazzoleni, C., Mei, F., Moffet, R. C., Nelson, D., Obland, M. D., Oetjen, H., Onasch, T. B., Ortega, I., Ottaviani, M., Pekour, M., Prather, K. A., Radney, J. G., Rogers, R. R., Sandberg, S. P., Sedlacek, A., Senff, C. J., Senum, G., Setyan, A., Shilling, J. E., Shrivastava, M., Song, C., Springston, S. R., Subramanian, R., Suski, K., Tomlinson, J., Volkamer, R., Wallace, H. W., Wang, J., Weickmann, A. M., Worsnop, D. R., Yu, X.-Y., Zelenyuk, A., and Zhang, Q.: Overview of the 2010 Carbonaceous Aerosols and Radiative Effects Study (CARES), Atmos. Chem. Phys., 12, 7647-7687, doi:10.5194/acp-12-7647-2012, 2012.